MATERIALS PHYSICS AND MECHANICS RESEARCH ARTICLE

**Submitted: July 8, 2025** **Revised: October 23, 2025** **Accepted: November 17, 2025**

# Microstructural and chemical features of a zinc-aluminum coating on high-strength eutectoid steel wire microalloyed with vanadium

**A.G. Korchunov [1], Yu.Yu. Efimova [1], K.G. Pivovarova [1]✉, A.Yu. Stolyarov [2], A.M. Yazvenko [2]**

[1] Nosov Magnitogorsk State Technical University, Magnitogorsk, Russia

[2] OJSK «Magnitogorsk hardware and sizing plant "MMK-METIZ", Magnitogorsk, Russia

✉ kgpivovarova@gmail.com

**ABSTRACT**

This paper presents a comprehensive study of the processes involved in applying zinc-aluminum coatings onto high-strength eutectoid steel wire microalloyed with vanadium. The study provides description of surface preparation methods, such as fluxing in $ZnCl_2$ and $FeCl_2$ solutions, followed by hot-dip galvanizing and zinc-aluminizing at elevated temperatures. Particular attention is given to microstructural analysis of the coatings using optical microscopy, scanning electron microscopy, and X-ray microanalysis. As a result, structural zones of the coatings, their elemental composition, thickness, and microhardness were identified. The research revealed that the zinc-aluminum coating structure consists of layers with different crystalline phases — namely η-, ζ-, and δ-phases — along with the presence of iron, aluminum, and zinc in various zones. Elemental distribution analysis across the wire cross-section confirmed coating homogeneity and internal diffusion. An important aspect of the work was the evaluation of microhardness changes in the steel core after coating application. This study contributes to the development of protective coating technologies for fasteners, expands understanding of the structure and properties of zinc-aluminum layers, and highlights the need for further improvements to enhance the stability and performance of protective coatings under operating conditions.

**KEYWORDS**

eutectoid steel microalloyed with vanadium • high-strength wire • galvanizing • microstructure coating zinc-aluminizing • phases • chemical composition • microhardness

**Citation:** Korchunov AG, Efimova YuYu, Pivovarova KG, Stolyarov AYu, Yazvenko AM. Microstructural and chemical features of a zinc-aluminum coating on high-strength eutectoid steel wire microalloyed with vanadium. *Materials Physics and Mechanics*. 2026;54(3): 32–41.
http://dx.doi.org/10.18149/MPM.5432026_3

## Introduction

In Russia and abroad, the production of metal products with various coatings that provide reliable protection against atmospheric corrosion and possess high consumer and aesthetic characteristics is actively developing [1–3]. In particular, wire with a zinc-aluminum coating is widely used in areas such as agriculture, construction, packaging, the automotive industry, and the production of wires for electric power transmission lines [4–7]. The production of rolled metal with zinc-aluminum coatings is developing due to the combination of the high corrosion resistance of zinc and the heat-resistant properties of aluminum [8–11].

Various solutions are available on the market that use the advantages of zinc-aluminum coatings to enhance the durability and reliability of metal products.

© A.G. Korchunov, Yu.Yu. Efimova, K.G. Pivovarova, A.Yu. Stolyarov, A.M. Yazvenko, 2026.
Publisher: Peter the Great St. Petersburg Polytechnic University
This is an open access article under the CC BY-NC 4.0 license (https://creativecommons.org/li-censes/by-nc/4.0/)

For example, Bekaert offers Bezinal zinc-aluminum coatings [12]. The Bezinal coating is a eutectoid alloy of zinc and aluminum (95 and 5 %, respectively) applied to steel wire in a hot state. The composition and coating application technology provide reliable anti-corrosion protection (approximately 2.5–3 times higher than that of galvanized wire with the same coating weight) and coating stability at high temperatures (up to 350 °C) [13].

One of the most common types of zinc-aluminum coating is the Galfan coating [14–18]. Galfan is widely used in the automotive industry due to its high corrosion resistance, excellent ductility, and good forming characteristics [19]. The Galfan coating contains approximately 5 wt. % aluminum, which is very close to the eutectoid point (6 wt. % Al) in the zinc-aluminum system, and also includes up to 0.05 wt. % rare earth metals such as lanthanum and cerium. The microstructure of the Galfan coating typically consists of two phases: a zinc-rich proeutectoid phase (with an aluminum content of less than 5 wt. %), surrounded by a eutectoid phase (with an aluminum content of 5–10 wt. %). The latter is formed by β-aluminum plates (with an aluminum content of 5–25 wt. %) and η-zinc plates (with an aluminum content of less than 5 wt. %) [20,21].

Zinc-aluminum coatings are considered effective in preventing the formation of brittle binary Fe–Zn intermetallic compounds at the interface between the zinc coating and the steel substrate. Instead, ternary Fe–Al–Zn intermetallic compounds, which exhibit significantly less brittleness, form in the transition layer. Furthermore, these compounds partially block the diffusion of zinc into the steel substrate and iron toward the zinc coating. Thus, the microstructure and composition of the intermetallic layer between the coating and the steel are of particular importance [22–31].

Recently, developments aimed at improving quality, reducing cost, and expanding the technological capabilities of applying zinc-aluminum coatings have been underway [23,24,32]. Nevertheless, the issue of long-term stability and corrosion resistance of these coatings remains relevant. In this regard, it is of interest to analyze the distribution of iron, aluminum, and zinc — which are components of the possible phases of the Fe–Al–Zn system — across the cross-section of the coated wire. The aim of this study is a comprehensive metallographic and elemental analysis of the structure, phase composition, and microhardness of zinc and zinc-aluminum coatings on wire made of 80F grade steel.

## Materials and Methods

Metallographic analysis of wire samples with zinc-aluminum coating was carried out at the laboratories of OJSC "Magnitogorsk Hardware and Sizing Plant "MMK-METIZ"" and Nosov Magnitogorsk State Technical University. The subject of the study was cold-drawn high-strength wire with a diameter of 2.59 mm (ultimate tensile strength of 2228 MPa) made of 80F grade steel, the chemical composition of which is presented in Table 1.

The wire was treated by fluxing in a solution of $ZnCl_2$ and $FeCl_2$ salts with concentrations of 91.5 and 6.5 g/dm³, respectively, at a temperature of 46 °C, followed by drying at 190 °C. Subsequently, the wire was sequentially subjected to hot-dip-

**Table 1.** Chemical composition of eutectoid steel microalloyed with vanadium

| Mass fraction of elements: maximum values or ranges (in wt. %) | | | | | | | | | | | |
|---|---|---|---|---|---|---|---|---|---|---|---|
| C | Si | Mn | P | S | Cr | Ni | Cu | N | Al | Ti | V |
| 0.800 | 0.300 | 0.730 | 0.020 | 0.020 | 0.100 | 0.100 | 0.100 | 0.008 | 0.005 | 0.005 | 0.100 |

galvanizing by immersion in a molten zinc bath at a temperature of 468 °C and to hot dip zinc-aluminizing at a melt temperature of 440 °C. The actual diameter of the wire after coating application was 2.67 mm.

The set of metallographic studies was carried out using a Zeiss Axio Observer light microscope with a Thixomet PRO computer image analysis system and a JSM-6490LV scanning electron microscope (SEM). The thickness and length of the coating zones were determined using the "Linear Dimension" tool in the Thixomet PRO system on electron microscopy images of the cross-sectional microstructure of the samples, which were imported into the software. Measurements were performed on at least 10–15 microstructural images of the studied samples. The relative measurement error did not exceed 5–7%. Energy-dispersive X-ray spectroscopy (EDS/EDX) using an INCA Energy 450X-MAX 50 system was employed to determine the qualitative and quantitative composition of the coating. The microhardness of the coating and the steel core was measured by indenting a diamond pyramid with an angle of 136° between opposite faces under a load of 1 kg using a Buehler Micromet 5103 microhardness tester, according to the Vickers hardness scale in accordance with GOST R ISO 6507-1:2005 "Metallic materials – Vickers hardness test – Part 1: Test method (IDT)".

## Results and Discussion

On the surface of the zinc and zinc-aluminum coating of the wire, a dendritic structure is visible. In the first case, it consists of almost pure zinc (Fig. 1(a,b)); in the second case,

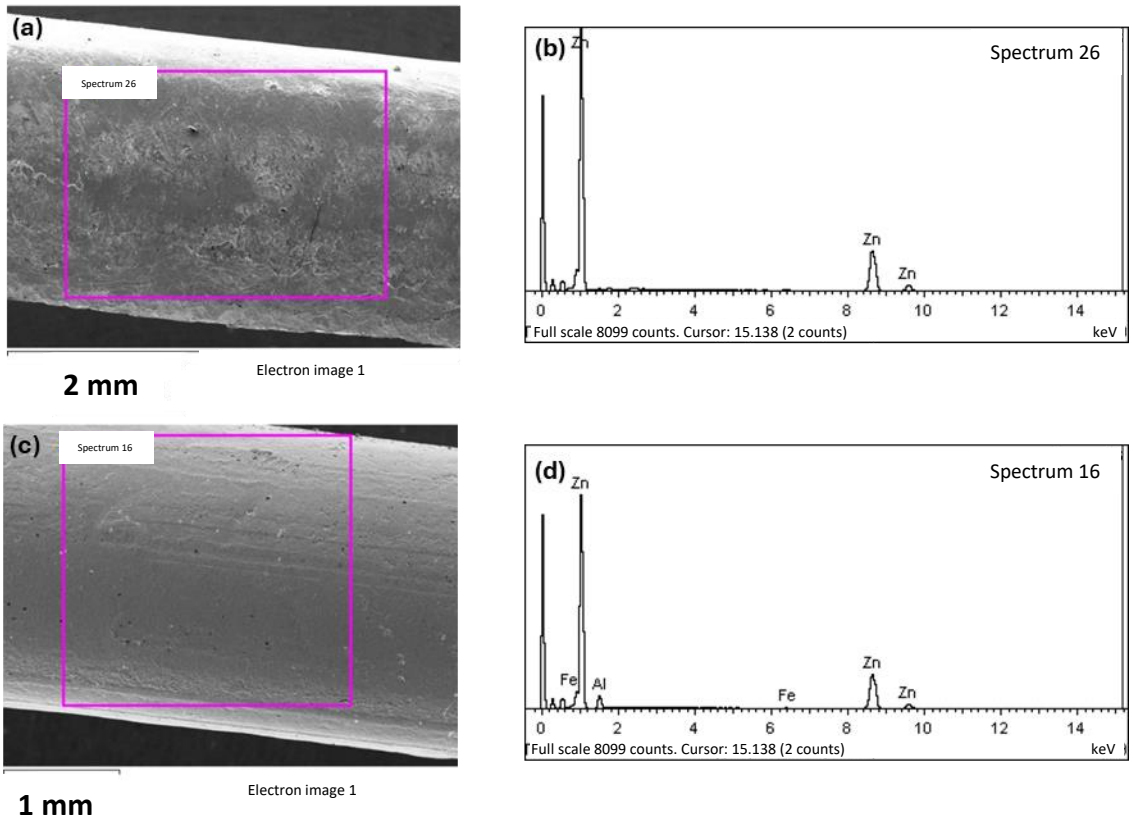



**Fig. 1.** Electron image of the wire surface with zinc (a) and zinc-aluminum coating (c) and X-ray microanalysis spectra (b, d) of the corresponding areas

it consists of zinc, aluminum, and iron (Fig. 1(c,d)). The microstructure of the studied zinc coating in the cross-section of the wire is shown in Fig. 2(a). Structurally, the following zones can be distinguished: an overlay layer (1) is observed on the surface, followed by a looser, more strongly etching layer (2), then a layer of dense columnar structure (3), and a dense layer bordering the steel substrate (4).

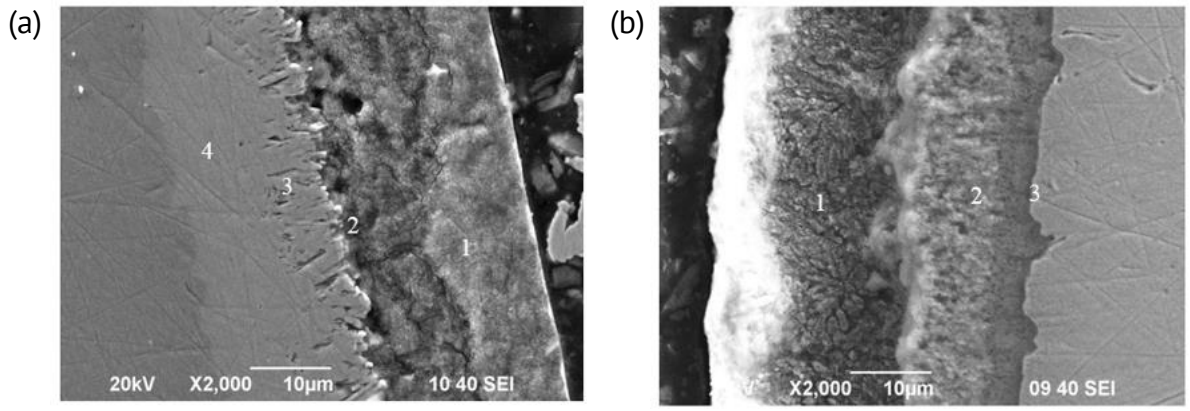



**Fig. 2.** Characteristic arrangement of crystalline zones of zinc (a) and zinc-aluminum (b) coating in the wire cross-section

The elemental composition of individual layers was determined in areas corresponding to the identified structural zones. The X-ray microanalysis results indicate that the X-ray spectra taken from the coating contain zinc peaks, which have the highest intensity, and iron peaks of lower intensity, while the spectra obtained from the steel substrate contain only iron and carbon peaks.

Analysis of the obtained results allows the conclusion that, in terms of chemical composition, structural zones 4, 3, and 1 (Fig. 2(a)) represent the δ-phase, ζ-phase, and η-phase (almost pure zinc), respectively (Table 2). Layer 2 consists of a mixture of the η-phase and a small amount of the ζ-phase, the crystals of which have grown into the overlay zinc layer. The Γ-phase and α-phase zones are not identified upon etching, which is apparently due to the small thickness of the transition diffusion zone between the steel substrate and the zinc coating. This is illustrated by the nature of the element distribution curves along the line, which indicate that the width of the transition zone is about 1 μm. Element distribution shows that zinc is distributed more or less uniformly across

**Table 2.** Elemental microanalysis, microhardness and extent of structural zones of the studied zinc coating

| Structural zones | Zone length, μm | Element content, % | | | | | | Microhardness, MPa | Assumed phase |
|---|---|---|---|---|---|---|---|---|---|
| | | Zn | | | Fe | | | | |
| | | min | max | average | min | max | average | | |
| Zone 1 | 2.26–11.69 | – | 100 | – | – | – | – | 887 | η |
| Zone 2 | 11.16–20.80 | 99.04 | 99.32 | 99.19 | 0.68 | 0.96 | 0.82 | | η+ζ |
| Zone 3 | 7.70–10.65 | 93.00 | 93.93 | 93.36 | 6.07 | 7.00 | 6.64 | 3567 | ζ |
| Zone 4 | 9.25–10.85 | 91.54 | 91.90 | 91.76 | 8.10 | 8.46 | 8.24 | | δ |

the coating cross-section, whereas iron diffuses quite well into zones 4 and 3 (δ-phase and ζ-phase) and, to a lesser extent, into zones 2 and 1 (η-phase of the zinc coating). The extent of individual coating zones is presented in Table 2, and the total coating thickness is 39.0–41.5 μm.

The microhardness of zones 1 and 2 was 887 MPa, while that of zones 3 and 4 was 3567 MPa. Determining the microhardness of individual zones was not possible due to their small extent. The microstructure of the studied zinc-aluminum coating in the cross-section of the wire is shown in Fig. 2(b). Structurally, the following zones can be distinguished: a layer with a dendritic structure (1) is observed on the surface, followed by a layer of dense columnar structure (2) and a dense layer bordering the steel substrate (3).

The elemental composition of individual layers was determined in areas corresponding to the identified structural zones. The X-ray microanalysis results indicate that the X-ray spectra taken from the coating contain zinc, aluminum, and iron peaks, while the spectra obtained from the steel substrate contain iron, manganese, and carbon peaks. Elemental analysis of the structural zones (Table 3) shows that the surface zone 1 contains the highest amount of zinc — approximately 83 % — and practically no iron, while zone 3, bordering the steel substrate, contains the highest amount of aluminum — approximately 50 %.

**Table 3.** Elemental microanalysis and extent of structural zones of the studied zinc-aluminum coating of the wire

| Structural zones | Zone length, μm | Element content, % | | | | | | | | | Micro-hardness, MPa | Assumed phase |
|---|---|---|---|---|---|---|---|---|---|---|---|---|
| | | Zn | | | Al | | | Fe | | | | |
| | | min | max | aver | min | max | aver | min | max | aver | | |
| Zone 1 | 22.31-34.80 | 70.69 | 89.19 | 82.48 | 9.90 | 28.66 | 17.03 | 0.47 | 0.91 | 0.66 | 3615 | α+β |
| Zone 2 | 8.10-16.71 | 52.5 | 58.5 | 56.15 | 32.21 | 35.19 | 33.50 | 9.16 | 12.31 | 10.25 | 2414 | $FeAl_3$, $Fe_2Al_5Zn_x$ and δ-phase, contenting Al |
| Zone 3 | 2.90-6.40 | 23.24 | 38.43 | 29.69 | 43.08 | 54.20 | 49.34 | 18.49 | 22.56 | 20.97 | | |

The microhardness of zone 1 was 3615 MPa, while the microhardness of zones 2 and 3 was 2414 MPa. Determining the microhardness of individual zones 2 and 3 was not possible due to their small extent. The extent of individual coating zones is presented in Table 3, and the total coating thickness is 43.3–54.1 μm.

Surface zone 1 presumably consists of two phases: a β-solid solution (almost pure zinc), which in this case contains up to 83 % Zn, and an α-solid solution based on aluminum. Moreover, as evidenced by the element distribution maps across the section of the specimen, the structure consists of alternating regions of β-solid solution rich in zinc, separated by interlayers of α-solid solution rich in aluminum. This structure of the surface coating layer provides reliable corrosion protection. The more active zinc matrix begins to corrode first, leaving the aluminum interlayers intact; therefore, the corrosion resistance of the coating does not decrease over time but rather increases.

The results of the study indicate that iron diffuses quite actively into the coating within zones 2 and 3. In these zones, the $FeAl_3$ phase is present, which forms first because the heat of formation of this compound is greater than the heat of formation of the iron-zinc Γ-phase and δ-phase. The δ-phase ($FeZnA1_3$) is also formed, as well as a phase based on $Fe_2Al_5$, which is identified as the $Fe_2Al_5Zn_x$ compound containing approximately 40 % Fe, 40 % Al, and 20 % Zn. The phase based on the $Fe_2Al_5$ compound prevents the reaction between iron and molten zinc and thereby also hinders the formation of intermediate iron-zinc compounds. The $Fe_2Al_5$ layer is very uniform in thickness and forms as a result of aluminum diffusion into the steel.

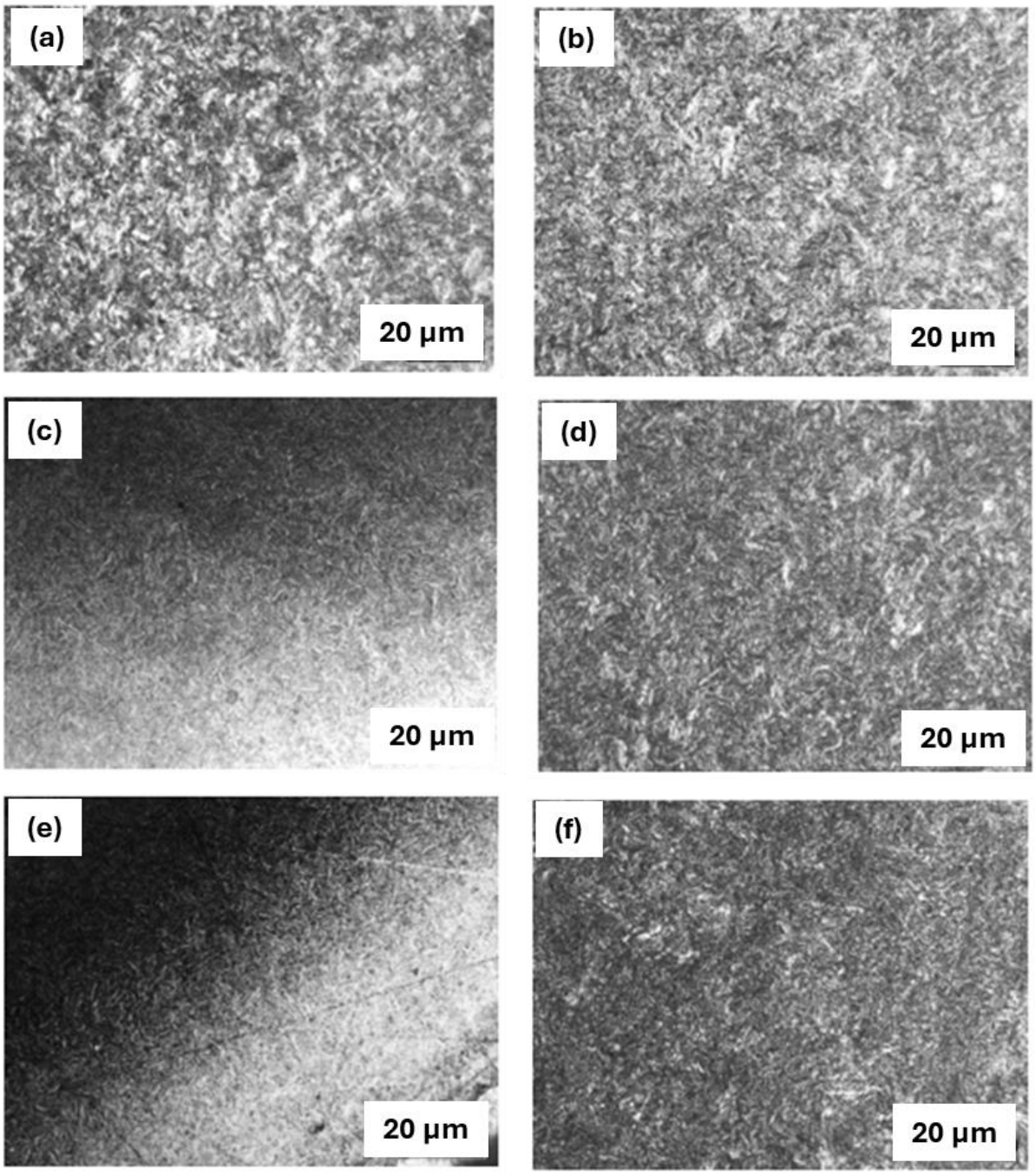



**Fig. 3.** Microstructure of steel wire after fluxing (a,b), galvanizing (c,d) and zinc-aluminizing (e,f); (a,c,e) surface of the steel wire; (b,d,f) central zone of the steel wire

The results of the element distribution analysis in the zones of the zinc-aluminum coating showed that zinc is present in all zones of the coating, and its content gradually increases with distance from the interface with the steel substrate, reaching a maximum value approximately in the center of surface zone 1, and then decreases somewhat upon further approach to the surface. The aluminum content, on the contrary, is highest in zone 3 adjacent to the substrate and decreases upon transition to zone 2 and then to zone 1, where it changes only slightly. The sharp drop in aluminum content at a distance of approximately 22 μm from the surface is associated with the presence of a step at the boundary between zones 1 and 2. The iron content decreases sharply in the transition zone from the steel substrate to the coating, then decreases slightly in zones 3 and 2, and is practically absent in surface zone 1.

The microstructure of the steel core of the wire is shown in Fig. 3. The structure in all samples is fairly uniform across the wire cross-section, has a vortex-like morphology characteristic of cold-drawn wire with high total reductions, and consists of deformed colonies of a ferrite-carbide mixture. No visible structural changes in the steel core microstructure after coating application are observed.

After coating application, a decrease in the microhardness of the steel core is observed: up to 17 % in the surface layers and up to 6 % in the central regions, compared to the microhardness after fluxing (Fig. 4). The decrease in microhardness can be explained by the relief of residual stresses and the occurrence of recrystallization processes, which began during hot-dip galvanizing at a bath temperature of 468 °C and during hot-dip zinc-aluminizing at a melt temperature of 440 °C. However, complete recrystallization cannot occur at these temperatures. The research results are used at OJSC "Magnitogorsk Hardware and Sizing Plant "MMK-METIZ"" in the development of production of high-strength and ultra-high-strength wire with zinc-based coatings, used for manufacturing cores of bare steel-aluminum conductors.

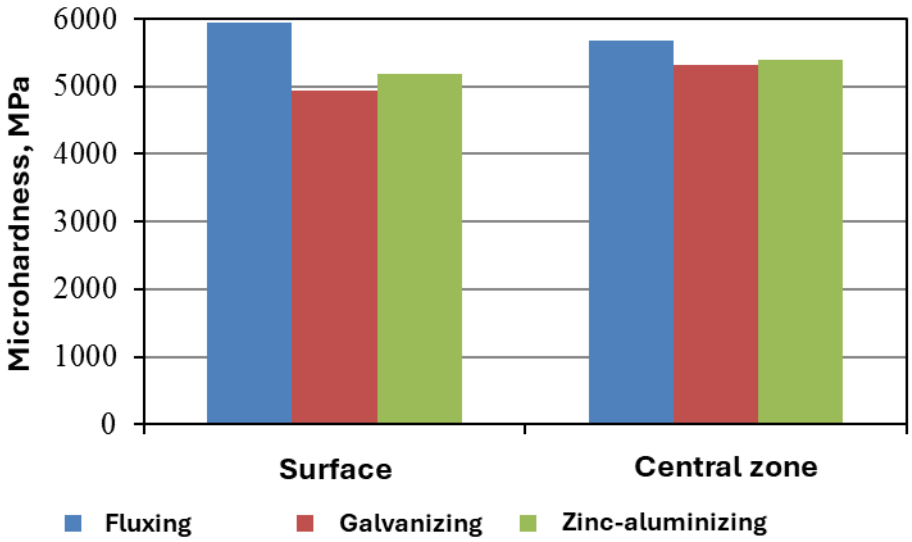



**Fig. 4.** Microhardness of steel wire after fluxing and coating application

## Conclusions

Based on the results of the study of the macro- and microstructure of the wire surface after fluxing and coating application, the following conclusions can be drawn:

1. Under the specified processing conditions, the zinc coating on the wire surface has a dendritic structure consisting predominantly of almost pure zinc (η-phase) with several intermetallic layers (δ, ζ). Element distribution shows uniformity of zinc throughout the coating and more active diffusion of iron into the δ and ζ zones, which is indicative of the nature of the diffusion processes and the coating structure.
2. The zinc-aluminum coating on the wire surface consists of three main zones: a surface dendritic layer (1), a dense columnar layer (2), and a dense layer adjacent to the steel substrate (3). Elemental analysis showed that zone 1 is dominated by zinc (up to 83%), while zone 3 is dominated by aluminum (approximately 50%), with iron present predominantly in the zones close to the substrate. The microhardness of the surface zone is higher (3615 MPa) than that of the inner zones (approximately 2414 MPa), which is associated with the different composition and phase constitution of the layers. The surface structure exhibits phases of the β-solid solution of zinc and the α-solid solution based on aluminum, which provide corrosion protection. Iron diffusion leads to the formation of $FeAl_3$, δ-phase, and $Fe_2Al_5Zn_x$ phases, which impede corrosion propagation.
3. The steel substrate of the cold-deformed high-strength wire retains a uniform microstructure of ferrite-carbide mixture after coating application, while the microhardness of the core in the cross-section decreases by 6–17% due to the relief of residual stresses and partial recrystallization during hot-dip galvanizing and zinc-aluminizing.

Overall, the study demonstrates the complex multilayer structure of the coatings, resulting from diffusion processes and phase transformations, as well as the influence of the melt composition on the microstructure, composition, and mechanical properties of the coatings and the wire core. These results make it possible to optimize the coating application technology to improve the wire's performance characteristics, including corrosion resistance and strength.

## Credit authorship contribution statement

**Aleksey G. Korchunov**: conceptualization, supervision, writing – review & editing; **Yuliya Yu. Efimova**: investigation, writing – original draft, data curation; **Ksenya G. Pivovarova**: investigation, writing – original draft, data curation; **Alexey Yu. Stolyarov**: resources, investigation, writing – review & editing; **Andrey M. Yazvenko**: resources, investigation, writing – review & editing.

## Conflict of interest

The authors declare that they have no conflict of interest.

## References

1. Zaytseva MV, Stolyarov AYu, Cherevichnaya MV. Analiz protsessa naneseniya tsink-alyuminiyevogo pokrytiya Galfan pri osvoyenii novoy tekhnologii goryachego tsinkovaniya na OAO «MMK-METIZ». *Chernyye Metally*. 2022;(1): 28–30. (In Russian)
2. Galchenko NK, Dampilon BV, Kolesnikova KA. Formation features of microstructure, elemental and phase compositions of the C-Cr-Mn-V-Fe coatings under conditions of electron beam (EB) surfacing in vacuum. *Materials Physics and Mechanics*. 2024;52(1): 142–149.
3. Gusev VM, Elagina OY, Volkov IV, Buryakin AV. Properties of 13% chromium wire electric arc spraying coatings. *Materials Physics and Mechanics*. 2021;47(4): 650–656.
4. Zorina YeA, Kim D, Naborshchikova DN. Osobennosti antikorroziynogo pokrytiya metallicheskikh mostov. In: *Nedelya Nauki ISI: Materialy Vserossiyskoy Konferentsii v 3-kh Chastyakh. Chast 2*. Sankt-Peterburg: Inzhenerno-Stroitelnyy Institut Sankt-Peterburgskogo Politekhnicheskogo Universiteta Petra Velikogo; 2021. p.311–314. (In Russian)
5. Zhan W, Li X, Qian X, Li Y, Ding Y, Zu Y, Xie F, Tian F. Preparation and characterization of synchronous chemical conversion coating on 6061 aluminum alloy/7075 aluminum alloy/galvanized steel substrates. *Metals*. 2022;12(12): 2011.
6. Zhu X, Shen Y, Ge Y, Zhang S. Effect of hot dip plating process parameters on microstructure and properties of zinc–10 % aluminum–mischmetal alloy coated for bridge cable steel wire. *Metals*. 2022;12(8): 1257.
7. Tarui T, Maruyama N, Eguchi T, Konno S. High strength galvanized steel wire for bridge cables. *Structural Engineering International*. 2002;12(3): 209–213.
8. Panchenko YuM, Marshakov AI, Nikolayeva LA, Nenasheva TA. Korrozionnaya stoykost pokrytiy tsink–alyuminiy i tsink–alyuminiy–magniy v razlichnykh regionakh mira. *Korroziya: Zashchita Materialov i Metody Issledovaniy*. 2023;(1): 21–55. (In Russian)
9. Rakhimov FA, Eshov BB, Ganiyev IN, Obidov ZR. Vliyaniye khroma na korrozionno-elektrokhimicheskiye svoystva tsinkovogo splava Zn5Al v neytralnoy srede. *Vestnik Pedagogicheskogo Universiteta (Yestestvennykh Nauk)*. 2021;2(10): 135–139. (In Russian)
10. Costa ANC, Silva GC, Ferreira EA, Nakazato RZ. Comparative analysis of corrosion resistance of zinc and Zn-Al-Mg coatings on carbon steel. *Research, Society and Development*. 2021;10(1): e49810111973.
11. Yemelyushin AN, Subbotina YuM. Proizvodstvo listovogo prokata s novymi korrozionnostoykimi pokrytiyami na osnove tsinka i alyuminiya v liniyakh AGNTs v usloviyakh PAO «MMK». In: *Sovremennyye Problemy i Napravleniya Razvitiya Metallovedeniya i Termicheskoy Obrabotki Metallov i Splavov*. 2022. p.53–59. (In Russian)
12. *Mega & Giga Strands for overhead power lines: Innovative solutions to power the future*. Available from: *https://www.bekaert.com/* [Accessed 8th August 2025]
13. Kutin LV. Vysokoprochnaya stalnaya provoloka s pokrytiyem Bezinal – resheniye dlya uvelicheniya propusknoy sposobnosti liniy elektroperedachi. In: *Linii Elektroperedachi 2008: Materialy Tretyey Rossiyskoy Nauchno-Prakticheskoy Konferentsii*. Krasnoyarsk; 2008. p.102–104. (In Russian)
14. Khezrloo A, Rezazadeh F, Rajaee M, Tayebi M, Aghaie E, Behnamian Y. Effect of coating parameters on microstructure, corrosion behavior, hardness and formability of hot-dip Galfan and galvanized coatings. *International Journal of Materials Research*. 2021;112(4): 321–332.
15. Zhang X, Leygraf C, Wallinder IO. Atmospheric corrosion of Galfan coatings on steel in chloride-rich environments. *Corrosion Science*. 2013;73: 62–71.
16. Fornalczyk A, Cebulski J, Dorota P. The morphology of corrosion products in FeAl alloys after heat-resistance tests at different temperatures. *Solid State Phenomena*. 2015;227: 409–412.
17. Mendala J. Influence of the cooling method on the structure of 55AlZn coatings. *IOP Conference Series: Materials Science and Engineering*. 2011;22: 012004.
18. Kania H, Komorowski L. The influence of the chemical composition of a zinc bath upon corrosion resistance of coatings obtained on Sebisty Steel. *Solid State Phenomena*. 2016;246: 85–90.
19. Kharrison D. Galfan – ekonomichnoye i prochnoye metallicheskoye pokrytiye. In: *Mir Metalla*. 2015. p.22–27. (In Russian)
20. Coni N, Gipiela ML, D'Oliveira ASCM, Marcondes PVP. Study of the mechanical properties of the hot dip galvanized steel and galvalume. *Journal of the Brazilian Society of Mechanical Sciences and Engineering*. 2009;13(4): 319–326.

21. Hayashida S, Mitsunobu T, Takebayashi H. Effect of Al in the coating layer of Zn-coated steel sheet on Zn oxidation during hot-stamping heating. *ISIJ International*. 2025;65(8): 1186–1191.
22. Zelechower M, Klis J, Augustyn E, Grzonka J, Stroz D, Rzychon T, Woznica H. The microstructure of annealed galfan coating on steel substrate. *Archives of Metallurgy and Materials*. 2012;57(2): 517–523.
23. Khaliq A, Kasva V, Alghamdi AS, et al. Iron intermetallic compounds (IMCs) formation mechanism in the molten aluminium zinc (Al-Zn) coating alloy. *Tehnicki Vjesnik*. 2024;31(2): 460–465.
24. Yadav M, Saha JK, Ghosh SK. Evaluation of corrosion behaviour of galvanised, galvalume and colour-coated steel sheets. *Archives of Metallurgy and Materials*. 2024;69(3): 865–879.
25. Pistofidis N, Vourlias G, Stergioudis G, et al. *Hot-dip galvanized and alternative zinc coatings*. Available from: *https://www.researchgate.net/publication/286284201_Hot-dip_galvanized_and_alternative_zinc_coatings* [Accessed 8th August 2025]
26. Han S-C, Sanchez DF, Grolimund D, Uhm S-H, Choi D-Y, Jeong H-Ch, Jun T-S. Role of silicon on formation and growth of intermetallic phases during rapid Fe–Zn alloying reaction. *Materials Today Advances*. 2023;18: 100368.
27. Shawki S, Hamid ZA. Effect of aluminium content on the coating structure and dross formation in the hot-dip galvanizing process. *Surface and Interface Analysis*. 2003;35(12): 943–947.
28. Bondareva OS. Vliyaniye temperatury i vremeni vyderzhki v rasplave na mikrostrukturu i fazovoye stroyeniye pokrytiya Zn + 7% Al na stalyakh razlichnykh marok. *Vestnik Sibirskogo Gosudarstvennogo Industrialnogo Universiteta*. 2025;1(51): 93–101. (In Russian)
29. Mesbahzadeh A, Abdolmaleki H, Seyedraoufi ZS, Mesbahzadeh A, Ahmadi A, Mirzavand K, Shajari Y, Bakhtiari H. Interfacial investigation of St13/molten Zn–5% Al and corrosion behavior of formed layer via hot-dip process. *Surface Engineering and Applied Electrochemistry*. 2021;57: 124–135.
30. Kato T, Nunome K, Kaneko K, Saka H. Formation of the ζ phase at an interface between an Fe substrate and a molten 0.2 mass % Al–Zn during galvannealing. *Acta Materialia*. 2000;48(9): 2257–2262.
31. Min T, Gao Y, Huang X, Gong Zh, Li K, Ma Sh. Effects of aluminum concentration on the formation of inhibition layer during hot-dip galvanizing. *International Journal of Heat and Mass Transfer*. 2018;127(C): 394–402.
32. Xu C, Teng H, Lv L, Han Yu, Jiang G, Liu H, Liu L. Experimental investigation and CALPHAD calculation concerning the effect of cooling rate and coating thickness on the industrial Al-Zn coated product. *JOM*. 2025;77: 5695–5706.